Journal of Catalysis **187,** 311–320 (1999)
Article ID jcat.1999.2627, available online at http://www.idealibrary.com on IDEAL®

Catalysis over Porous Anodic Alumina Film Catalysts with Different Pore Surface Concentrations

G. Patermarakis[1] and N. Nicolopoulos

Section of Materials Science and Engineering, Department of Chemical Engineering, National Technical University of Athens, Greece

Received January 4, 1999; revised June 29, 1999; accepted June 30, 1999

The catalytic behaviour of porous anodic Al_2O_3 films with different surface concentrations and lengths of pores vertical to the surface was investigated in the HCOOH decomposition test reaction in which they showed an ≅100% dehydrative action. The surface density and length of pores and the position on the pore walls were found to affect strongly the kinetic parameters activation energy, preexponential factor, and total and specific activity at each constant reaction temperature, revealing a strong catalytic heterogeneity of the pore wall surface. Anodic aluminas modified by hydrothermal treatment showed a much different catalytic behaviour, a strong reduction of the pore wall surface heterogeneity, and much higher activities than those of nonmodified aluminas. The promotion factor gave a maximum at a pore length specific for each pore surface density, usually increased with reaction temperature and generally varied between ≅3 and ≅23. Methods to prepare ultraactive aluminas of designed structure are thus predicted.

Key Words: **porous anodic alumina; designed structure; pore surface concentration; formic acid; catalytic decomposition.**

INTRODUCTION

The application of nonporous (1–7) and porous (8–17) anodic Al_2O_3 films in catalysis research as catalysts, as models for catalysts, substrates, and the porous structure of catalysts (9, 10, 12–17), and for comparing the adsorption–desorption methods for the determination of pore size distribution (11) has been recently investigated and the results were promising (18).

Porous anodic Al_2O_3 films were tested in the HCOOH decomposition reaction (15–17) which was employed in view of its previous widespread use as a model reaction for catalytic selectivity (19–21). The anodic Al_2O_3 exerts a much higher dehydrative catalytic efficiency than that of γ-Al_2O_3 chemically prepared (15). A new semi-industrial, multitubular, coaxial, catalytic reactor made of anodized aluminium with catalytic walls consisting of porous anodic alumina films was studied by the same test reaction (16). The structural features of porous anodic aluminas like thickness, porosity, and real surface were found to vary significantly with the preparation conditions (17). This, together with the existence of strict relationships (22) between the preparation conditions and the basic structural features, the pore surface concentration, and the pore base diameter, showed that the variable structure of porous anodic aluminas is well designed. Anodic alumina films with identical pore surface concentration and different pore base diameters and lengths of pores, nonmodified and modified by hydrothermal treatment, were tested in the above test reaction where they showed a very important catalytic behaviour while a new mechanism of the HCOOH dehydration reaction on alumina was proposed. Nevertheless, new material is necessary to fully elucidate the catalytic behaviour of anodic aluminas.

The change of pore surface concentration (even small), which depends solely on current density (22), exerts a strong effect on structural features like porosity, real surface, and maximum limiting pore length (17, 23, 24). It also affects significantly the thickness of the pore wall material at pore bases and along the pores (17, 24) and, as expected, the nature/composition of this material. The new idea of this work is that the investigation of the catalytic properties of anodic aluminas with different pore surface densities can yield the new material necessary to fully elucidate their catalytic behaviour. Anodic alumina films with different surface densities and lengths of pores and comparable pore base diameters were tested in the above test reaction to discover the effect of the pore surface density and of the relevant structure and nature characteristics and necessarily the effect of the pore length at each pore surface density (see later) on their catalytic behaviour. A new method to study the pore wall surface heterogeneity of porous anodic aluminas was developed. These catalysts modified by hydrothermal treatment were also tested and the promotion of catalytic activity was investigated. All new material, the pore wall surface heterogeneity, and the entire catalytic behaviour of anodic aluminas were interpreted and elucidated by their characteristic structure and nature.

[1] To whom correspondence should be addressed.

0021-9517/99 $30.00

EXPERIMENTAL

The materials and procedure for the preparation of porous anodic alumina catalysts were exactly the same as those reported in detail previously (17). Anodic alumina films were prepared in a nonstirred bath of 15% w/v H_2SO_4 at a bath temperature of 30°C. Since the pore surface density depends solely on current density (22, 24), different apparent current densities 5, 15, and 35 mA cm^{-2} were used to produce films with different pore surface densities, 3.69×10^{10}, 2.93×10^{10}, and 2.30×10^{10} cm^{-2}, correspondingly (24). As will be seen later even that relatively slight variation of pore surface density can reveal very important information.

Because the catalytic properties of anodic aluminas vary with the film thickness or the pore length (see later), the examination of their catalytic properties at different film thicknesses for each pore surface density is necessary. Different anodic oxidation times were used to produce different film thicknesses between low values, 1.5, 4.6, and 10.8 μm, and the maximum limiting attainable values at these current densities, i.e., 7.5, 20, and 38 μm, correspondingly (17).

The experimental setup, the procedure, and the experimental conditions of the catalytic decomposition of HCOOH, which was employed as a test reaction over anodic aluminas also in the present study, were the same as those described in detail previously (17). The range of reaction temperatures employed was 270–390°C and the drying temperature of the anodic aluminas used was up to 390°C. Nevertheless, in the present study a rate of scanning operation of the temperature range $\cong$2°C/min, which is lower than that used previously $\cong$2.5°C/min (17), was employed; this was done in order to obtain as accurate as possible measurements of reaction rate during the third scanning up operation of the temperature range, the reaction rate measurements of which were taken into consideration, by avoiding completely phenomena of hysteresis in the reaction rate measurements and phenomena of deactivation of catalysts which always occur during the initial stages of catalysis experiments. Also, to avoid any probable (even slight) effect of the dilution of HCOOH in the container of reactor by the product H_2O on the measurements, i.e., in cases of very high rates of HCOOH decomposition, the HCOOH was always replaced by new, pure HCOOH at the initiation of the third temperature scanning procedure. After catalysis experiments, the catalysts were modified by hydrothermal treatment in distilled, boiling H_2O at 100°C and tried similarly in the test reaction. The procedures of catalyst modification and catalysis experiments with modified catalysts were the same as previously reported (17).

RESULTS AND DISCUSSION

1. *Characterisation of the Structure and Nature/Composition of the Employed Porous Anodic Al_2O_3 Film Catalysts, Nonmodified and Modified*

In order to ensure that the results of catalysis experiments will be easily followed and understood, it was judged that a brief description of the characteristic structure and nature/composition of porous anodic aluminas, both nonmodified and modified, is necessary.

The structure of porous anodic Al_2O_3 films is characterised as a close-packed array of approximately hexagonal, columnar cells, each of which contains an elongated, roughly cylindrical pore extending between the film's external surface and the Al_2O_3–Al interface, where it is sealed by a thin, compact, hemispherical shell-shaped barrier-type oxide layer (25–27). The structural features, pore diameter, cell/pore surface density, etc., depend on the kind of electrolyte (28) and the conditions of the anodic oxidation of Al (24, 26, 27). The real pore shape depends on these conditions and is usually that of a cylinder, truncated cone, trumpet, etc. (24, 29). At the employed preparation conditions it is approximately that of a truncated cone (24).

This structure was elaborated by many works (9–12, 16, 25–28) and different methods like transmission electron microscopy (TEM) (9–12, 16, 28) and scanning electron microscopy (9). Pore size distributions, determined by TEM (9–12) and nitrogen adsorption–desorption methods (11), were narrow enough at each distance from pore bases so that the pores can be considered parallel and similar with uniform diameters along their length or across the film. The pore shape was deduced by TEM (9–12), the adsorption–desorption method (11), and a method consisting of the combined use of BET surface measurements and suitable mathematical models for the real surface derived from the kinetics of growth and structure of anodic aluminas (24). The surface densities, geometry, and sizes of pores of aluminas prepared at different conditions were determined elsewhere (17, 24) by this complex but reliable (17) method.

The dependence of various physical and structural features like film mass (m) spread over the 33 cm^2 oxidized geometric surface of the Al substrate or on the geometric surface of the oxide film catalyst (S_g), the film thickness, or the pore length (since the thickness of barrier layer is negligible in comparison to that of porous layer (24, 25)) (h), the porosity, the total real surface (S), and the specific real surface ($s = Sm^{-1}$) of catalysts prepared at many different conditions on the bath temperature, current density (j), and time (t) of the anodic oxidation of Al for catalysts preparation was described elsewhere (17). The h and S values of catalysts used here (Table 1) were obtained from that work for conditions of catalysts' preparation identical to those of

TABLE 1

Values of the Average Integrated (Over the Whole Pore Wall Surface Area) Kinetic Parameters Activation Energy (E) and Preexponential Factor (k_0) Reduced Per Unit of Geometric Surface Area (S_g) and of Pore Wall Real Surface Area (S) ($k_0S_g^{-1}$ and k_0S^{-1}, Correspondingly) Derived from the Catalytic Dehydration of HCOOH on the Employed (a) Nonmodified Porous Anodic Alumina Film Catalysts Prepared at Different Current Densities (j) (and Therefore with Different Pore Surface Densities (n)) and Different Anodic Oxidation Times (t) (and Therefore with Different Film Thicknesses or Pore Lengths (h) and Real Surfaces (S)) and (b) on the Modified Porous Anodic Alumina Film Catalysts

No. of catalyst	j (mA cm^{-2})	$10^{-10}n$ (cm^{-2})	t (min)	h (μm)	S (m^2)	E(Kcal mol^{-1})		log($k_0S_g^{-1}$/mol s^{-1}m^{-2})		log(k_0S^{-1}/mol s^{-1}m^{-2})	
						(a)	(b)	(a)	(b)	(a)	(b)
1	5	3,69	10	1.5	0.22	28.6	36.4	5.98	9.48	4.15	7.66
2	5	3,69	20	3.1	0.47	25.6	35.7	4.98	9.50	2.83	7.35
3	5	3,69	40	6.2	1.04	30.1	35.2	7.04	9.61	4.54	7.11
4	5	3,69	60	7.0	1.20	30.4	33.1	7.33	8.95	4.77	6.39
5	5	3,69	80	7.5	1.24	33.8	34.1	8.53	9.32	5.95	6.74
6	5	3,69	100	7.5	1.24	33.4	34.0	8.36	9.29	5.78	6.71
Mean values for catalysts 5 and 6						33.6	34.0	8.44	9.30	5.86	6.73
7a	15	2,93	10	4.6	0.49	26.2	34.3	5.02	8.66	2.85	6.49
7b	15	2,93	10	4.6	0.49	31.9		7.14		4.97	
8a	15	2,93	20	9.3	1.05	26.6	34.4	5.35	9.17	2.85	6.67
8b	15	2,93	20	9.3	1.05	27.1		5.61		3.11	
9	15	2,93	40	17.5	2.27	33.0	35.9	8.08	10.10	5.25	7.26
10	15	2,93	60	20.0	2.75	34.3	36.3	8.88	10.33	5.96	7.41
11	15	2,93	80	20.0	2.75	33.9	35.3	8.80	9.97	5.86	7.03
12	15	2,93	100	20.0	2.75	34.0	36.9	8.88	10.56	5.94	7.62
Mean values for catalysts 10–12						34.1	36.2	8.85	10.29	5.82	7.35
13a	35	2,30	10	10.8	1.00	32.8	33.2	7.21	8.65	4.72	6.17
13b	35	2,30	10	10.8	1.00	29.9		6.47		3.99	
14a	35	2,30	20	21.6	2.21	34.3	34.9	8.14	9.63	5.32	6.80
14b	35	2,30	20	21.6	2.21	30.9		6.92		4.10	
15a	35	2,30	30	32.5	3.66	33.7	32.9	8.71	9.22	5.66	6.18
15b	35	2,30	30	32.5	3.66	33.4		8.59		5.55	
16	35	2,30	50	38.0	4.77	33.9	32.2	9.16	9.08	6.00	5.92
17	35	2,30	75	38.0	4.77	33.1	32.8	8.92	9.27	5.73	6.08
18	35	2,30	100	38.0	4.77	34.0	31.0	9.17	8.53	5.98	5.34
Mean values for catalysts 16–18						33.6	32.0	9.08	8.96	5.90	5.78

this study. Generally, h and S increase with t and up to a t value specific for each j. Then they acquire maximum limiting values. The same is valid for the m and s parameters (17).

The pore base diameter (D_b) depends solely on the anodic oxidation temperature (temperature around pore bases during the oxide growth) (22). The pore/cell surface density (n) depends solely on j (22, 24). The D_b and n values of films prepared at the bath temperature and current densities identical to those of this study were determined elsewhere ((17) and (24), respectively). These are $D_b = 356$, 335, and 352 Å and $n = 3.69 \times 10^{10}$, 2.93×10^{10}, and 2.30×10^{10} cm^{-2}, respectively, at $j = 5$, 15, and 35 mA cm^{-2}. The pore mouth diameters in films with the maximum limiting thickness (h_c) equals the cell width (D_c) which depends solely on n. This diameter is $D_c = 603$, 676, and 763 Å, respectively, at the above j's (17). The corresponding thickness of barrier layer, $2^{-1}(D_c - D_b)$, becomes 124, 171, and 206 Å.

The anodic alumina is essentially a dry material containing a small amount of H_2O, either as H_2O or as OH^- and H^+, at a percentage $\leq 1\%$ (24, 30). Traces of the metal impurity compounds may be incorporated in the compact oxide bulk while stoichiometric defects may appear inside it (31). The compact pore wall material consists of microcrystallites the size of which is ≤ 25 or 40 Å (28, 32). Electrolyte anions, SO_4^{2-} in the present case, are always incorporated in the compact pore wall oxide, especially in intercrystalline surfaces (26–28, 33).

Considering the barrier layer or the pore wall material around the pore bases, the local average crystallite size increases from the pore base surface toward the oxide–Al

interface and the cell boundaries (28), i.e., with decreasing the true current density across the barrier layer during the oxide growth; the SO_4^{2-} local bulk concentration is significant near the surface and varies according to a bell-like distribution across the oxide; a maximum appears at a position inside it and then decreases strongly and becomes $\cong 0$ near the oxide–Al interface or the cell boundaries (33). These variations of crystallite size and of SO_4^{2-} bulk concentration across the barrier layer are extrapolated along the pore surface of the film with h_c thickness from the bases towards the mouths of pores for a thin oxide layer with thickness comparable to crystallite sizes.

During hydrothermal treatment of porous anodic Al_2O_3, H_2O either as OH^- and H^+ or as H_2O species is uptaken. At prolonged treatment and for $j = 5$–35 mA cm^{-2} the percentage of water uptake varies from 18–9.5% of the initial oxide mass for the lower thickness films used here up to 24.7–19.4% for the h_c thickness films (30). The H_2O uptake results in the hydration of oxide and the closure of pores as previously (30) described. The higher amount of the incorporated SO_4^{2-} ions is removed from the intercrystalline surfaces and OH^-, H^+ and H_2O are adsorbed on them (34). A hydrated skin layer develops on the pore wall surface, which becomes thicker with time, yielding a swollen layer which, considering, i.e., a h_c thickness film, at prolonged treatment closes up the pores completely up to a pore length lower than, but generally comparable to, h_c (30). The previously existing distribution of crystallite sizes is destroyed inside the hydrated layer on the pore walls and a "mixing" of crystallites of various sizes occurs at each point on the pore walls and along the pore wall surface while only a small amount of SO_4^{2-} may remain inside it.

During heating, as in catalysis experiments, the retained OH^-, H^+ and H_2O are removed almost completely (30). The swollen layer shrinks causing the movement/rearrangement of crystallites towards their initial positions and the reformation of pores with dry pore wall material again. The average crystallite size at each position on the pore walls is now higher than that of nonmodified oxide. This difference diminishes from the bases towards the mouths of the pores.

2. *Decomposition of HCOOH on Anodic Al_2O_3 Film Catalysts with Different Pore/Cell Surface Concentrations and Pore Lengths*

The initial deactivation of catalysts, until reliable measurements could be obtained, was significant being always ≤ 57, 58, and 87% for $n = 3.69 \times 10^{10}$, 2.93×10^{10}, and 2.30×10^{10} cm^{-2}, respectively. Its nature was explained previously (17). The reaction rate (r) measurements, obtained at different temperatures (T), refer to the total amount of oxide present on the 33 cm^2 geometric surface area of the Al_2O_3 film catalyst. The decomposition of HCOOH on all the used catalysts (nonmodified and modified) was $\cong 100\%$ dehydration ($HCOOH \rightarrow CO + H_2O$). The apparent reaction order in the experimental conditions, determined as described previously (17), was zero. Due to the zero order of reaction, reaction rate yields directly the reaction rate constant (k).

From the r values at different T's for each catalyst, the Arrhenious plots $\ln k$ vs $10^3\ T^{-1}$ were constructed. They were always good straight lines with correlation coefficient ≥ 0.9972. The kinetic parameters, activation energy (E), and preexponential factor (k_0) reduced per m^2 of geometric surface area ($k_0 S_g^{-1}$) and per m^2 of real surface area ($k_0 S^{-1}$) were determined (Table 1). Since the r values concern the whole pore wall surface of each catalyst, the kinetic parameters E and $k_0 S^{-1}$ are the integrated average ones over this surface. At each n, E and $k_0 S^{-1}$ vary similarly, i.e., increase or decrease together; this is known as the compensation effect (20, 21), usually observed when the nature and structure of catalysts remain basically similar and change slightly, i.e., with the preparation conditions etc., and the reaction mechanism does not change.

The reproducibility is generally good for catalysts with the maximum thickness, h_c, at all n's. At $n = 3.69 \times 10^{10}$ cm^{-2} and low h's, minima in the kinetic parameters appear. This is also valid for the average values of kinetic parameters at $n = 2.93 \times 10^{10}$ cm^{-2}. At each n the kinetic parameters become maximum for the h_c thickness catalysts. At $n = 2.30 \times 10^{10}$ cm^{-2} the average values seem to increase slightly with h while comparable values are observed for the two lower h's catalysts. This predicts that at low h's, minima in their values may appear for this n as well. For catalysts with the same thickness at different n's, the kinetic parameters increase with n. The h_c thickness catalysts gave comparable kinetic parameters at all n's.

Three activities can be defined, the rS_g^{-1} (total activity) and the rm^{-1} and rS^{-1} (specific activities). Of specific importance appears to be the examination of the variation of the rS_g^{-1} and rS^{-1} activities with h and S correspondingly. The rS_g^{-1} vs h and rS^{-1} vs S plots at $T = 350$°C and different n's are shown in Figs. 1a and 1b. A ring-shaped differential surface area at a position on the pore wall surface of the average pore, $(nS_g)^{-1}dS$, is considered. The local reaction rate yielded by this surface is $(nS_g)^{-1}dr$. The local specific activity of this differential surface is therefore $[(nS_g)^{-1}dr]/[(nS_g)^{-1}dS] = dr/dS$. The variation of this local specific activity with S is determined as follows: The rS^{-1} vs S plots can be approximated satisfactorily by parabolas, as shown in Fig. 1b,

$$rS^{-1} = a + bS + cS^2 \quad \text{or} \quad r = aS + bS^2 + cS^3, \qquad (a > 0, b < 0, c > 0), \quad [1]$$

where $a = 18.9 \times 10^{-7}$, 8.8×10^{-7}, and 4.7×10^{-7} mol s^{-1} m^{-2}, $b = -35.4 \times 10^{-7}$, -8.6×10^{-7}, and -3.6×10^{-7} mol s^{-1} m^{-4} and $c = 24.3 \times 10^{-7}$, 3.1×10^{-7}, and 1.1×10^{-7} mol s^{-1} m^{-6}, respectively, for $n = 3.69 \times 10^{10}$, 2.93×10^{10}, and

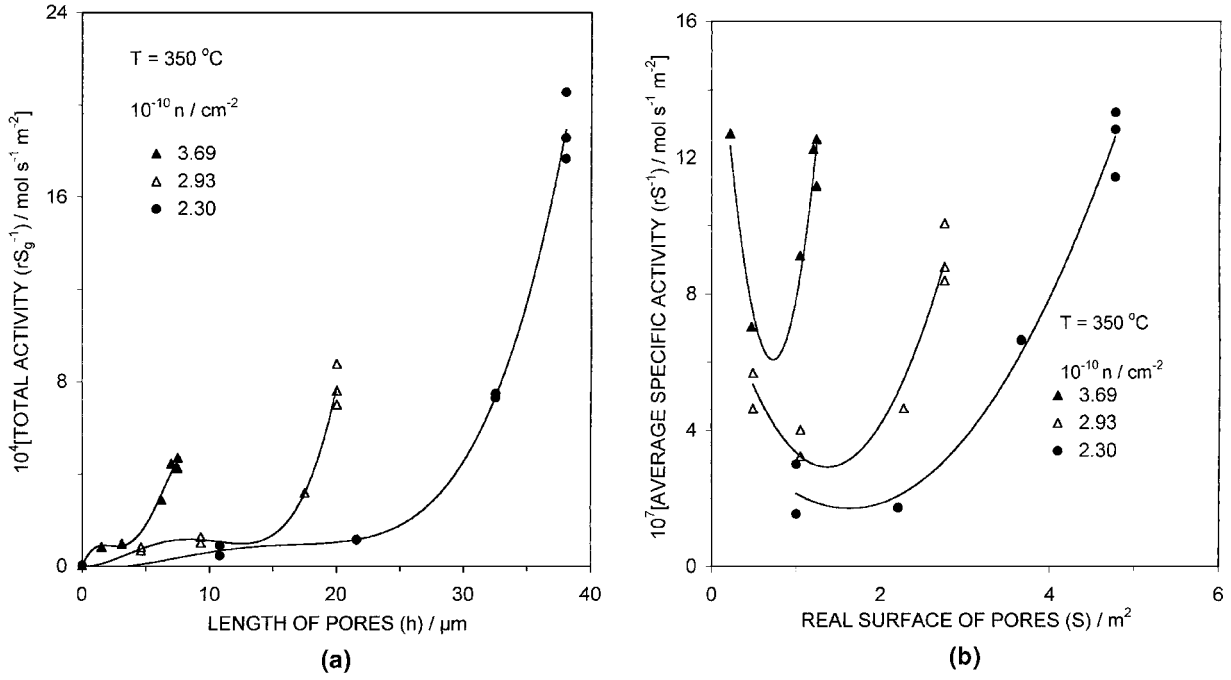

FIG. 1. Variation (a) of the total activity rS_g^{-1} (reaction rate, r, reduced per unit of geometric surface area, S_g, of anodic alumina film catalyst) with film thickness or pore length (h) and (b) of the average specific activity rS^{-1} with the pore wall real surface area of catalyst (S) in the catalytic dehydration of HCOOH at reaction temperature $T = 350°C$ on porous anodic alumina catalysts with pore surface densities 3.69×10^{10}, 2.93×10^{10}, and 2.30×10^{10} cm^{-2}.

2.30×10^{10} cm^{-2}. Then, dr/ds becomes

$$dr/dS = a + 2bS + 3cS^2, \qquad [2]$$

which is also a parabola. The dr/ds vs S plots defined by Eq. [2] at the above n's are shown in Fig. 2. The integrated average specific activity rS^{-1} has a minimum at a position where $d(rS^{-1})/dS = 0$, i.e., at $S_1 = -b(2c)^{-1}$. The local specific activity dr/ds has also a minimum at a position where $d(dr/dS)/dS = d^2r/dS^2 = 0$, i.e., at $S_2 = -b(3c)^{-1}$. Hence, the position S_2 lies between the pore base and the position S_1. From S_1, S_2, and the h vs S plots, constructed by the h and S values of Table 1, the positions S_1 and S_2 were found to lie at relative pore lengths from pore bases $hh_c^{-1} = 0.61$, 0.58, and 0.45 and $hh_c^{-1} = 0.42$, 0.41, and 0.32, respectively, for the above n's. The variations of E, k_0S^{-1}, rS^{-1}, and dr/dS with h or S show a strong pore wall surface heterogeneity largely affected by n, h, and the position on pore walls. The above analysis also constitutes a new interesting method for investigating the pore wall surface heterogeneity of anodic aluminas.

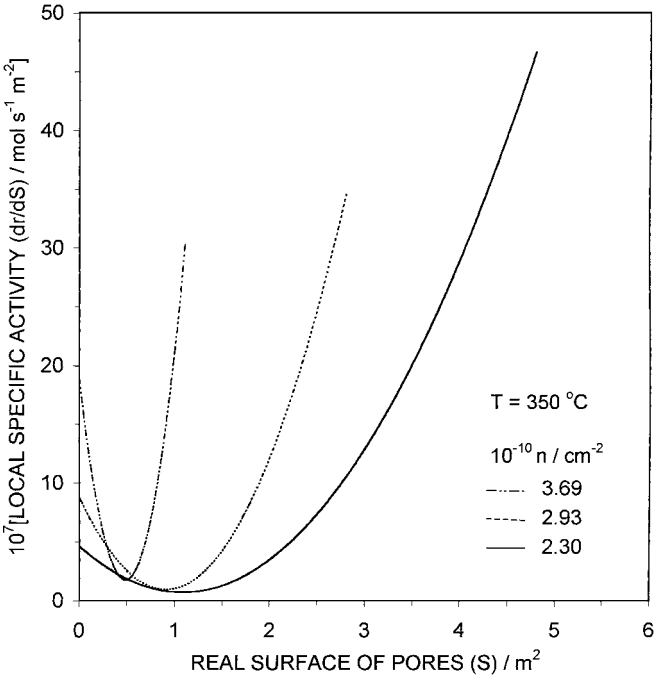

FIG. 2. Variation of the local specific activity $[(nS_g)^{-1}\,dr]/[(nS_g)^{-1}\,dS] = dr/dS$ (differential reaction rate, $(nS_g)^{-1}\,dr$, reduced per unit of the corresponding ring-shaped differential surface area, $(nS_g)^{-1}\,dS$, on the pore wall surface) with the real pore wall surface area (S) in the catalytic dehydration of HCOOH at reaction temperature $T = 350°C$ on porous anodic alumina catalysts with pore surface densities 3.69×10^{10}, 2.93×10^{10}, and 2.30×10^{10} cm^{-2}.

3. Decomposition of HCOOH on the Modified Anodic Al_2O_3 Film Catalysts

The initial deactivation of catalysts, until reliable measurements of reaction rate could be obtained, was generally lower than that of the nonmodified catalysts being always

$\leq$33, 55, and 65% for $n = 3.69 \times 10^{10}$, 2.93×10^{10}, and 2.30×10^{10} cm^{-2}, respectively. Its nature, which is different from that of nonmodified catalysts, was explained previously (17). All Arrhenius plots were accurate straight lines. The correlation coefficient varied always between 0.9983 and 0.9997. This was higher and the reproducibility was better than those of nonmodified catalysts.

The derived kinetic parameters are cited in Table 1. The span of their variation at each n is much lower than that of nonmodified catalysts. Although, on average, a slight decrease of parameters with h at $n = 3.69 \times 10^{10}$ cm^{-2}, a slight increase at $n = 2.93 \times 10^{10}$ cm^{-2}, and a slight fluctuating variation (or a slight on average decrease) at $n = 2.30 \times 10^{10}$ cm^{-2} are observed, they can be considered roughly comparable for the various h's at each n. At $n = 3.69 \times 10^{10}$ and 2.93×10^{10} cm^{-2} and for the h_c thickness catalysts these parameters are slightly higher than those of nonmodified catalysts while at $n = 2.30 \times 10^{10}$ cm^{-2} these are, on average, slightly lower than those of nonmodified catalysts. The differences in the kinetic parameters between modified and nonmodified catalysts at $n = 3.69 \times 10^{10}$ and 2.93×10^{10} cm^{-2} become generally higher at the lower h's. For modified catalysts with the same h, kinetic parameters usually increase with n. For the h_c thickness catalysts at different n's, the kinetic parameters show a clear maximum at $n = 2.93 \times 10^{10}$ cm^{-2} and are lower at $n = 2.30 \times 10^{10}$ cm^{-2}.

The variations of rS_g^{-1} and rS^{-1} activities with h and S, respectively, are shown in Figs. 3a and 3b. The dependence of rS^{-1} on S is completely different from that of nonmodified catalysts, Figs. 1b and 3b. Only at $n = 3.69 \times 10^{10}$ cm^{-2} the rS^{-1} vs S plots show minima in both cases, but at S values different for modified and nonmodified catalysts. Nevertheless, in the case of modified catalysts, taking into consideration the experimental error, a continuous decrease of rS^{-1} with S can be supposed and, in actual fact, this minimum may be apparent and not true.

4. Promotion of Catalytic Efficiency Effected by Modification of Catalysts

Comparison of activities, Figs. 1a and 3a, shows a strong promotion of catalytic efficiency effected by modification. The ratio of the rate of reaction on modified catalysts to that on nonmodified catalysts, promotion factor (pf), varies with h at four constant T's, 330, 350, 370, and 390°C, as shown in Fig. 4. At each n, pf gives a maxima at an h value depending on n. At $n = 3.69 \times 10^{10}$ and 2.93×10^{10} cm^{-2} and $h < h_c$, pf increases with T and the differences become maximum at the h's where maxima in the pf values appear. At the lowest n, the pf values at each h are generally comparable for all T's. The maximum pf value at each T decreases with n. For the h_c thickness catalysts at each n, the pf values at the different T's are comparable; these are also neighbouring at $n = 3.69 \times 10^{10}$ and 2.93×10^{10} cm^{-2} and slightly lower at $n = 2.30 \times 10^{10}$ cm^{-2}. At each pair

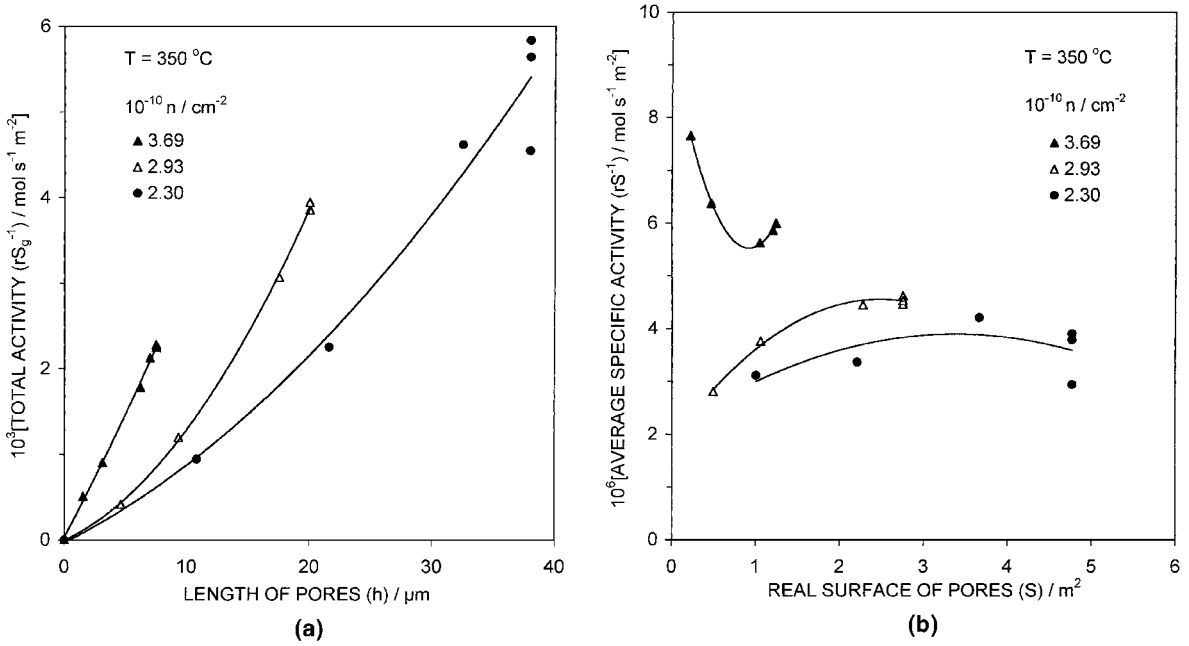

FIG. 3. Variation (a) of the total activity rS_g^{-1} (reaction rate, r, reduced per unit of geometric surface area, S_g, of anodic alumina film catalyst) with film thickness or pore length (h) and (b) of the average specific activity rS^{-1} with the pore wall real surface area of anodic alumina (S) in the catalytic dehydration of HCOOH at reaction temperature $T = 350$°C on the modified porous anodic alumina catalysts with pore surface densities 3.69×10^{10}, 2.93×10^{10}, and 2.30×10^{10} cm^{-2}.

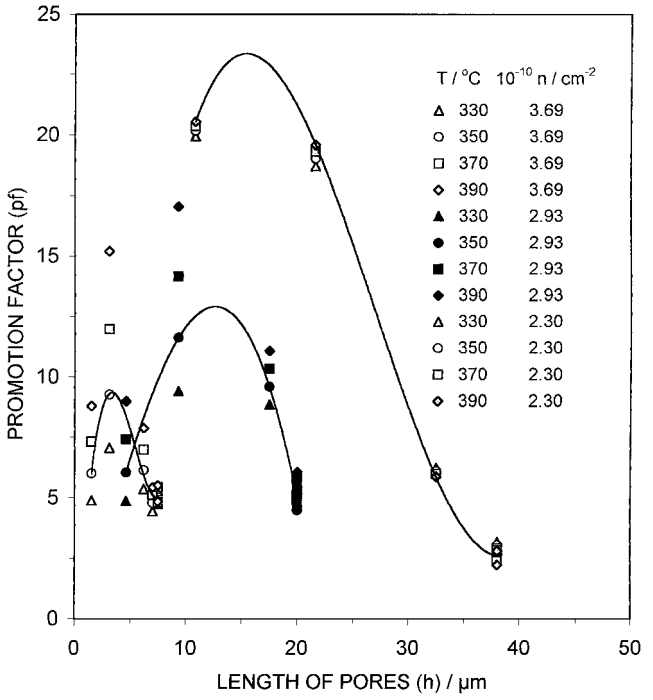

FIG. 4. Variation of promotion factor (ratio of the rate of catalytic reaction on the modified anodic alumina catalyst to that on the nonmodified anodic alumina catalyst) at reaction temperatures $T = 330$, 350, 370, and 390°C with pore length (h) for catalysts with pore surface densities 3.69×10^{10}, 2.93×10^{10}, and 2.30×10^{10} cm^{-2}. Lines in the plots correspond to the results obtained at reaction temperature $T = 350$°C.

of T and h values, pf generally decreases strongly with n except for a region of low h's at $n = 2.93 \times 10^{10}$ cm^{-2}, where between $n = 3.69 \times 10^{10}$ and $n = 2.93 \times 10^{10}$ cm^{-2} the trend is reversed.

5. Interpretations

5.1. Interpretation of the catalytic behaviour of nonmodified anodic alumina catalysts. Previously (21) it was suggested that the catalytic dehydration of HCOOH on chemically prepared γ-Al_2O_3 takes place by an acid–base mechanism through the adsorption of HCOOH molecules on Lewis acidic sites (Al^{3+}) to which the HCOOH molecules are bound through the oxygen atoms of hydroxyl groups. The catalytic decomposition of HCOOH on chemically prepared γ-Al_2O_3 at relatively low reaction temperatures $\leq$190°C yielded also an almost complete dehydration (35–37). It was supported that HCOOH generally decomposes in two stages. In the initial transient stage the dissociative adsorption of HCOOH yields $HCOO^-$ and H^+ adsorbed on Al^{3+} and O^{2-} sites, respectively, HCOOH decomposes by the collision of HCOOH in the gaseous phase with the adsorbed $HCOO^-$ species, and the product H_2O is strongly bound on the Al^{3+} active sites which are thus destroyed. In the stationary state HCOOH decomposes by the collision of HCOOH molecules and Bronsted acidic sites, i.e., the H^+ supplied to O^{2-} sites as above, and the reaction is also inhibited by the product H_2O.

The HCOOH decomposition on anodic alumina (17) at temperatures 270–390°C, which are much higher than the above, showed that HCOOH decomposes by another mechanism which entails: (i) dissociative adsorption of HCOOH on the surface of microcrystallites accessible to HCOOH molecules, yielding H^+ and $HCOO^-$, adsorbed on O^{2-} and Al^{3+} sites correspondingly, which saturate this surface (fast step); (ii) decomposition of $HCOO^-$ yielding CO which easily desorbs (slow step); (iii) condensation of neighbouring OH^- groups into H_2O which easily desorbs in the reaction temperature range (fast step). This different mechanism is justified by the much different nature/composition and structure of anodic aluminas than those of chemically prepared ones. This mechanism offers a good tool assisting the interpretation of the new material of this study and the full elucidation of catalytic behaviour of anodic aluminas.

The local specific activity dr/dS varies along the pore wall surface of a film with the maximum thickness (Fig. 2) in a way opposite to that of the surface concentration of SO_4^{2-}. It seems that in the region of the pore wall surface enriched by SO_4^{2-} the effect of the variation of the SO_4^{2-} surface concentration on the activity is generally higher than that of crystallite sizes. Only from a point lying between the position where the SO_4^{2-} surface concentration is maximum and the pore mouth's position, where the SO_4^{2-} surface concentration becomes $\cong$0, the main effect on the local activity at each position must be exerted by the local average crystallite size.

The opposite variations of the SO_4^{2-} surface concentration and of the local activity along the pore wall surface show that: (i) the positions along the pore wall surface where the maximum in the SO_4^{2-} surface concentration and the minimum in dr/dS appear must be almost identical; (ii) the SO_4^{2-} ions hinder the reaction since evidently they occupy catalytically active Al^{3+} sites; (iii) the selectivity of reaction does not change, and only the local activity decreases when the local SO_4^{2-} surface concentration increases, since the SO_4^{2-} ions exhibit also some dehydrative efficiency but much lower than that of the A^{3+} sites; it is well known that the SO_4^{2-} ions in H_2SO_4 solutions cause almost exclusively dehydration of HCOOH-producing CO (laboratory method for CO preparation); (iv) the very low dr/dS value at the S_2 position implies an almost complete saturation of crystallite surfaces by SO_4^{2-} at this position; probably this does not occur before heating during catalysis experiments, but it does during heating as a result of digestion of crystallites to some small extent, especially at this position.

Because the total pore base surface per unit of S_g, $2^{-1}n\pi D_b^2$, decreases with j (22) and the total Al-Al_2O_3 interface surface per unit of S_g, $2^{-1}n\pi D_c^2$, is independent

of j (23), the true current density at both surfaces also increases with j. Then, the average crystallite sizes at both surface regions decrease with j or increase with n. The bulk SO_4^{2-} concentration must increase with j or decrease with n at the pore base region and be almost independent of j or n in the maximum concentration region inside the barrier layer. Hence, on average across this layer, the crystallite sizes increase and the SO_4^{2-} concentration decreases with n. This is also valid on average along the pore wall surface of the h_c thickness catalysts.

The shift of both the r/S and dr/dS vs S plots generally upwards on increasing n, with some insignificant exception in the dr/dS vs S plots at some low S values (Figs. 1b and 2) must be attributed mainly to the decrease of both the average and the local surface SO_4^{2-} concentration in films with the same S. The value of dr/dS for S tending to the maximum limiting one, or the specific activity around the pore mouth's region where the SO_4^{2-} surface concentration is $\cong 0$, decreases with n or with increasing crystallite size and the factor which exclusively affects the activity is the average crystallite size. This reveals the effect of crystallite size on the local catalytic behaviour of oxide along the pores. The minimum in the rS^{-1} value of the h_c thickness catalysts around $n = 2.93 \times 10^{10}$ cm^{-2} is then the result of the opposite effects of the average crystallite size and of the average SO_4^{2-} surface concentration. In this way at each S and h value the variations of the activities rS^{-1} and rS_g^{-1}, respectively, with n are also well explained.

When the Arhenius equation is applied on a ring shaped differential surface area at a position on the pore walls, $(nS_g)^{-1}dS$, it is inferred that the variation of the local E (E_l) and of the local k_0 reduced per unit of surface ($k_{0,s,l}$), which must be very close to dk_0/dS, with S at each n is similar to that of dr/dS and the compensation effect occurs along the pore wall surface.

The variation of E_l and $k_{0,s,l}$ with h or S and the compensation effect between E_l and $k_{0,s,l}$ at each n show that: (i) the surface density and intensity of active sites is variable along the pore wall surface; (ii) at each position on the pore walls, with a $(nS_g)^{-1}dS$ ring-shaped differential surface area, a distribution of the active sites, as regards the enthalpy of adsorption of HCOOH and the activation energy of $HCOO^-$ decomposition, occurs; (iii) at each position as above the higher is the density of active sites and therefore the $k_{0,s,l}$, the higher is the average enthalpy of HCOOH adsorption and therefore the E_l, as it is inferred from the activated complex theory; (iv) the decrease of the average crystallite size at a position causes the increase of the number of active sites and of the local average enthalpy of HCOOH adsorption and therefore of the local activation energy of $HCOO^-$ decomposition; (v) the SO_4^{2-} ions occupy a large number of active surface sites and preferably those with the higher adsorption enthalpy and activation energy.

The variation of crystallite sizes along the pore wall surface from the bases towards the mouths of pores causes a decrease of both E_l and $k_{0,s,l}$. The variation of the SO_4^{2-} surface concentration along this surface yields minima in E_l and $k_{0,s,l}$ at a position along the pores. Since the effect of the SO_4^{2-} surface concentration is generally stronger than that of crystallite sizes, the trend of the variation of both E_l and $k_{0,s,l}$ is that effected by the variation of the SO_4^{2-} surface concentration. The variation of the integrated average E and k_0S^{-1} with h is then easily justified. The opposite actions of these factors on average along the pore surface of the h_c thickness catalysts almost balance each other at different n's yielding neighbouring E and k_0S^{-1} values.

5.2. Interpretation of the catalytic behaviour of modified anodic alumina catalysts. The extent of oxide modification depends on the extent of its hydration which, in turn, depends on both the pore base diameter D_b and the thickness of oxide at pore bases, $2^{-1}(D_c - D_b)$. The oxide thickness necessary for complete closure of pores around their bases during hydration (30) is found from the swelling factor (sf), i.e., the ratio of the volume of the swollen hydrated oxide to the initial volume of the nonhydrated oxide. This thickness is $\cong 2^{-1}\ D_b/\text{sf}$. Since $\text{sf} \cong 1.5$ (27), it is $\cong$119, 112, and 117 Å, respectively, at $n = 3.69 \times 10^{10}$, 2.93×10^{10}, and 2.30×10^{10} cm^{-2}.

It is comparable to the barrier layer thickness only at $n = 3.69 \times 10^{10}$ cm^{-2} and on prolonged treatment both the oxide hydration, even around the pore base region, and the removal of the incorporated SO_4^{2-} are complete or almost complete. The only factor determining the catalytic behaviour of the pore wall surface oxide in this case is the crystallite size. Even if a complete mixing of crystallites with different sizes at each position on the pore walls is supposed during hydration and swelling of the pore wall oxide, the average crystallite size across it will increase towards the pore mouths. This is valid for both the new pore wall surface and the active sublayer adjacent to the surface which are formed during heating in catalysis experiments. The local kinetic parameters must decrease towards the pore mouths and therefore the average kinetic parameters E, k_0S^{-1}, and rS^{-1} must also decrease with h. Because of the relatively thin pore wall material at this n, the average crystallite sizes of modified and nonmodified oxides at each position on the pore walls and mainly towards the pore mouths, where the surface area becomes significant due to the conical pore shape and exerts a significant effect on the catalytic behaviour of the whole surface, must be comparable. Then, the E and k_0S^{-1} parameters of nonmodified and modified catalysts with h_c thickness are expected to differ slightly, as indeed is observed.

For the other two n's it is evident that the positions where the pore wall oxide can be completely hydrated and released almost completely from SO_4^{2-} on prolonged

treatment lie well beyond the pore base. From the above sf value these are calculated to be at a distance $\cong 0.21\ h_c$ and $\cong 0.26\ h_c$ away from the pore base at $n = 2.93 \times 10^{10}$ and $2.30 \times 10^{10}\ cm^{-2}$, correspondingly. The oxide may swell also in unison along the pores towards the pore mouths and the real lengths of pores filled by hydrated material may be appreciably higher than the above. However, a part of the SO_4^{2-} ions still existing in the nonhydrated layer probably diffuses during heating in catalysis experiments to the modified (and almost free of SO_4^{2-}) layer which becomes again "poisoned" by the transferred SO_4^{2-} ions and those already existing in small amounts inside it.

Irrespective of the SO_4^{2-} concentration variation across the barrier layer and along the pore wall surface of nonmodified oxides, due to the conical pore shape, both the thickness of the remaining nonhydrated layer (17, 30) and the average SO_4^{2-} concentration inside it decrease towards the pore mouths. This is valid also for the SO_4^{2-} concentration in the whole modified layer and the active sublayer on pore walls during heating. Since the effect of SO_4^{2-} on the catalytic effectiveness is stronger than that of crystallite sizes, an increase of the aforementioned kinetic parameters with h is generally expected, as is indeed observed at $n = 2.93 \times 10^{10}\ cm^{-2}$.

At $n = 2.30 \times 10^{10}\ cm^{-2}$ the nonhydrated layer is relatively longer and on average thicker. The average SO_4^{2-} bulk concentration in the modified layer during heating becomes higher than that at the other n's. But the on-average significantly lower crystallite sizes and the consequent significantly higher intercrystalline surface area prevent, to some extent, the above secondary poisoning of the active sublayer on pore walls by the SO_4^{2-} diffusion. The effect of the SO_4^{2-} concentration variation along the pores becomes slightly lower than, or almost balances, the effect of crystallite size variation. That is why the rS^{-1} activity increases only slightly or exhibits a just observable maximum and E and k_0S^{-1} are slightly fluctuating (but comparable) or on average slightly decreasing with h or S. Similarly, the observed variations of all kinetic parameters with h, S, and n are easily explained.

5.3. Interpretation of the variation of promotion factor. During modification the on-average largest aforementioned changes in the oxide nature/composition and structure, related to the removal of the SO_4^{2-} species, occur in films for which the average SO_4^{2-} surface concentration along the pores is the maximum. Approximately these are the films which give minima in rS^{-1} (Fig. 1b). The slight and large variations of rS^{-1} with S (or h) for the modified and nonmodified, respectively, catalysts at each n justify satisfactorily the pf vs h plots profile. The variation of pf with T and n at each constant h is similarly explained by the variations of, i.e., rS^{-1} with T and n for modified and nonmodified catalysts.

CONCLUSIONS

From the results of this study the following concluding remarks can be drawn:

1. The designed structure of porous anodic aluminas, defined by the surface density and length of pores and the distribution of the thickness of pore wall material along the pores, affects strongly their, almost completely dehydrative, catalytic behaviour in the employed test reaction.

2. The heterogeneity of oxide along the pore wall surface depends strongly on the pore surface density, the pore length, and the position on the pore wall surface. It results in a significant variation of catalytic effectiveness and kinetic parameters. A new method was developed for describing this heterogeneity and revealing the main factors which create the heterogeneity and explain the catalytic behaviour of anodic aluminas.

3. The modification of anodic aluminas by hydrothermal treatment reduces strongly the pore wall surface heterogeneity at each pore surface density and results in both a significant change of kinetic parameters and a much higher catalytic efficiency. The pf value at a constant T (i.e., 350°C) gives a maximum at an intermediate h specific for each n, generally increases with decreasing n, and varies between $\cong 3$ and $\cong 23$. Usually T exerts a positive effect on pf.

4. The results of the present study predict the manners to prepare ultra-active aluminas of designed porous structure and optimise their catalytic dehydrative efficiency. These render the anodic aluminas very important materials usable as models for catalysts or substrates.

5. Since the catalytic behaviour of the anodic aluminas and the main structure and nature characteristics affecting their behaviour were well elucidated, the same test reaction may be suitable to characterise the catalytic properties of anodic aluminas prepared at different pore forming electrolytes, conditions, etc., and correlate these properties with their nature and structure.

REFERENCES

1. Ruckenstein, E., and Malhotra, M., *J. Catal.* **41**, 303 (1976).
2. Chu, Y., and Ruckenstein, E., *J. Catal.* **55**, 281 (1978).
3. Ruckenstein, E., and Chu, Y., *J. Catal.* **59**, 109 (1979).
4. Chen, J., and Ruckenstein, E., *J.Catal.* **69**, 254 (1981).
5. Glassl, H., Kramer, R., and Hayek, K., *J. Catal.* **63**, 167 (1980).
6. Glassl, H., Kramer, R., and Hayek, K., *J. Catal.* **68**, 388 (1981).
7. Glassl, H., Hayek, K., and Kramer, R., *J. Catal.* **68**, 397 (1981).
8. Glassl, H., and Hayek, K., *Thin Solid Films* **89**, 413 (1982).
9. Rai, K., and Ruckenstein, E., *J. Catal.* **40**, 117 (1975).
10. Chu, Y., and Ruckenstein, E., *J. Catal.* **41**, 384 (1976).
11. Ihm, S. K., and Ruckenstein, E., *J. Colloid Interface Sci.* **61**, 146 (1977).
12. Ihm, S. K., and Ruckenstein, E., *IEC Prod. Res. and Dev.* **17**, 110 (1978).
13. Honicke, D., *Appl. Catal.* **5**, 197 (1983).
14. Honicke, D., *Appl. Catal.* **5**, 199 (1983).

15. Skoulikidis, Th., and Sarropoulos, C., *in* "Proceedings of 4th International Congress for the Study of Bauxites, Alumina, and Aluminium," Vol. 3, p. 356. National Technical University, Athens, 1978.
16. Skoulikidis, Th., and Patermarakis, G., *Aluminium* **65**, 185 (1989).
17. Patermarakis, G., and Pavlidou, C., *J. Catal.* **147**, 140 (1994).
18. Cocke, D. L., Johnson, E. D., and Merill, R. P., *Catal. Rev. Sci. Eng.* **26**, 163 (1984).
19. Trillo, J., Munuera, G., and Griado, J., *Catal. Rev.* **7**, 51 (1973).
20. Bond, G., "Catalysis by Metals." Academic Press, London, 1962.
21. Krylov, O., "Catalysis by Nonmetals." Academic Press, London, 1970.
22. Patermarakis, G., and Moussoutzanis, K., *J. Electrochem. Soc.* **142**, 737 (1995).
23. Patermarakis, G., and Moussoutzanis, K., *Electrochim. Acta* **40**, 699 (1995).
24. Patermarakis, G., Lenas, P., Karavassilis, Ch., and Papayiannis, G., *Electrochim. Acta* **36**, 709 (1991).
25. Keller, F., Hunter, M. S., and Robinson, D. L., *J. Electrochem. Soc.* **100**, 411 (1953).
26. Young, L., "Anodic Oxide Films." Academic Press, London, (1961).
27. Diggle, J., Downie, T., and Goulding, C., *Chem. Rev.* **69**, 365 (1969).
28. Thompson, G. E., Furneaux, R. C., and Wood, G. C., *Corros. Sci.* **18**, 481 (1978).
29. Patermarakis, G., and Tzouvelekis, D., *Electrochim. Acta* **39**, 2419 (1994).
30. Patermarakis, G., and Kerassovitou, P., *Electrochim. Acta* **3**, 125 (1992).
31. Bernard, W. J., and Russel, P. G., *J. Electrochem. Soc.* **127**, 1256 (1980).
32. Baker, P., and Pearson, R., *J. Electrochem. Soc.* **119**, 160 (1972).
33. Parkhutic, V. P., *Corros. Sci.* **26**, 295 (1986).
34. Marphy, J., *in* "Proceedings, Anodizing Aluminium Symposium, Birmingham, UK," p. 3. Aluminium Development Association, London, 1967.
35. Noto, Y., Fukuda, K., Onishi, T., and Tamaru, K., *Trans. Faraday Soc.* **63**, 2300 (1967).
36. Fukuda, K., Noto, Y., Onishi, T., and Tamaru, K., *Trans. Faraday Soc.* **63**, 3072 (1967).
37. Tamaru, K., "Dynamic Heterogeneous Catalysis." Academic Press, London, 1978.